Mobile Networks and Applications (2023) 28:4–18
https://doi.org/10.1007/s11036-022-01993-9

Deterministic Wireless Channel Characterization towards the Integration of Communication Capabilities to Enable Context Aware Industrial Internet of Thing Environments

Imanol Picallo[1,2] · Peio López Iturri[1,2] · Mikel Celaya-Echarri[3] · Leyre Azpilicueta[3] · Francisco Falcone[1,2]

Accepted: 27 September 2021 / Published online: 27 May 2022

Abstract
In order to provide interactive capabilities within the context of Internet of Thing (IoT) applications, wireless communication systems play a key role, owing to in-herent mobility, ubiquity and ease of deployment. However, to comply with Quality of Service (QoS) and Quality of Experience (QoE) metrics, coverage/capacity analysis must be performed, to account for the impact of signal blockage as well as multiple interference sources. This analysis is especially complex in the case of indoor scenarios, such as those derived from Industrial Internet of Things (IIoT). In this work, a fully volumetric approach based on hybrid deterministic 3D Ray Launching is employed providing precise wireless channel characterization and hence, system level analysis of indoor scenarios. Coverage/capacity, interference mapping and time domain characterization estimations will be derived, considering different frequencies of operation below 6 GHz. The proposed methodology will be tested against a real measurement scenario, providing full flexibility and scalability for adoption in a wide range of IIoT capable environments.

Keywords Industrial internet of things · 3D ray launching · Coverage/capacity estimations · Time domain estimations

1 Introduction

Industrial environments are evolving to achieve Industry 4.0 paradigms, supported by communication, computing and robotic capabilities provided by the Industrial Internet of Things (IIoT) or Cyber physical Systems (CPS), among others. In this context, communication systems play key role providing collaborative, context-aware environments, with high levels of interactivity, whilst considering the specific requirements in terms of data integrity, delay, security or interoperability of industrial applications [1, 2]. As a function of application and system requirements, different communication systems can be employed, combining traditional field buses with transport networks providing service to Supervisory Control and Data Acquisition (SCADA) systems or telemetry and tele control applications, combining wired/wireless networks [3]. Wireless communication systems are gaining popularity, owing to rapid deployment, inherent mobility and scalability [4]. The evolution in communication systems is enabling to optimize network device implementation or tactile internet applications based on the use of edge/fog computing approaches [5, 6], or the implementation of delay constrained services with the aid of capabilities in 5G such as ultra-reliable low latency communications [7].

However, their adoption is challenging owing to different factors such as high propagation losses and unstable links, owing to large density of scatterers and elements leading to obstruction, interference or security vulnerabilities [8–12]. The expected increase in the number of transceivers leads to a reduction in cost, form factor and energy consumption, posing new challenges in terms of operation cycle design, energy efficient link control and routing and the use of energy harvesting strategies [13]. An increase in node density, as expected from the massive deployment of transceivers in IoT enabled environments, demands a reduction in overall device cost, which can potentially impact in a negative way in system operation, owing to factors such as

✉ Francisco Falcone
francisco.falcone@unavarra.es

1 Electrical, Electronic and Communication Engineering Department, Public University of Navarre, Pamplona, Spain

2 Institute of Smart Cities, Public University of Navarre, 31006 Pamplona, Spain

3 School of Engineering and Sciences, Tecnologico de Monterrey, 64849 Monterrey, Mexico

reduced receiver sensitivity or non-optimal antenna configurations, which increase overall interference levels. This is opening the path of exploring new mechanisms to optimize the operation of IIoT systems, such as federated learning strategies [14] or the use of artificial intelligence to optimize wireless link operation [15]. In this way, new capabilities such as multi robot operation [16] or enhanced tracking and localization techniques [17], among others can be adopted. In this context, the analysis of wireless channel characterization and its impact on overall system operation is necessary to provide adequate Quality of Service (QoS) and Quality of Experience (QoE) metrics [18, 19]. Wireless system design can hence benefit with the adoption of different strategies, mainly in layers 1 to 3, with the definition of functionalities such as dynamic spectrum access [20], delay aware routing protocols [21], link scheduling and cooperative transmission schemes [22, 23], traffic offload mechanisms [24], to name a few.

1.1 Wireless channel characterization in IIoT scenarios

When considering the limitation in the use of wireless communication systems in industrial applications, the impact of interference is one of the main issues, decreasing coverage/capacity relations and delay metrics mainly due to an increase in retransmissions. As the number of coexisting technologies and the density of transceivers increase, interference impact is more significant [25–27], so characterizing interference is relevant to envisage potential mitigation mechanisms [28]. In this sense, different approaches have been proposed, such as the use of cognitive radios [29] or enhanced interference identification aided by fuzzy neural networks [30]. Moreover, large signal variability owing to shadowing effects given by large clutter densities can also degrade system performance, with larger percentage of non-line of sight and partial line of sight communication links. Given therefore limitations imposed by interference and signal variability, especially in the case of indoor scenarios, wireless channel modelling and characterization is compulsory to perform radio planning tasks, related with wireless network/node topology and configuration. Different models have been proposed within the framework of 3GPP [31–33], following different approaches such as 3D geometric stochastic models in industrial environments [34], modelling in mm-wave frequency ranges [35], the consideration of human body motion within indoor scenarios [36], or polarization diversity [37, 38].

In the specific case of industrial environments, wireless channel characterization has been enriched by multiple measurement-based test campaigns in wide range of frequency bands, considering different aspects such as large-scale propagation, shadowing or time varying signals [39–45]. Further works have proposed wireless channel mapping and measurement techniques [46, 47], modelling within 5G NR FR1 bands [48–51], mm-wave frequency bands [52, 53], ultra-wide band channels [54] the study of delay constrained networks [55], or the effect in localization systems [56]. Different applications and industrial scenarios have been considered, such as petroleum plants, automobile plants, office and factories scenarios [57–60].

In this work, the characterization of complex indoor scenarios amenable to industrial environments will be performed to obtain accurate estimations of coverage/capacity frequency/power values, interference mapping and time domain characteristics. Full details of the indoor scenario will be taken into account and results for the complete volume of the scenario under test will be derived, thanks to the use of deterministic volumetric in-house implemented channel modelling approach. In this way, it is feasible to provide a full volumetric characterization of the wireless channel behavior, in terms of desired transmitted signals as well as mapping of arbitrary interference sources. This enables to provide coverage/capacity estimations within scenarios with high clutter densities, such as industrial environments, which in turn aid in device as well as network planning phases. The proposed methodology enables to perform wireless channel characterization with high accuracy, enabling the consideration of any required transceiver location and variation in the characteristics of the scenario, such as variable densities and distributions of objects, such as stocked goods or raw materials. The rest of the work is organized

Table 1 Material Properties for the Elements within the Scenario under Test

Parameter	Relative Permittivity (ε_r)	Conductivity (σ) [S/m]
Metal	4.5	$37.8*10^6$
Plastic	8.5	0.02
PVC	4	0.12
Glass	6.06	0.11
Brick wall	4.44	0.11

Table 2 D Ray Launching simulation parameters

Frequency of Operation	433 MHz, 868 MHz, 2.4 GHz, 3.5 GHz
TX Power	0–22 dBm
Antenna Type/Gain	Monopole/0 dB
Angular Resolution ($\Delta\phi = \Delta\theta$)	1°
N (maximum reflections to extinction)	6
Cuboids size (Mesh resolution)	10 cm × 10 cm × 10 cm
Diffraction phenomenon	Activated

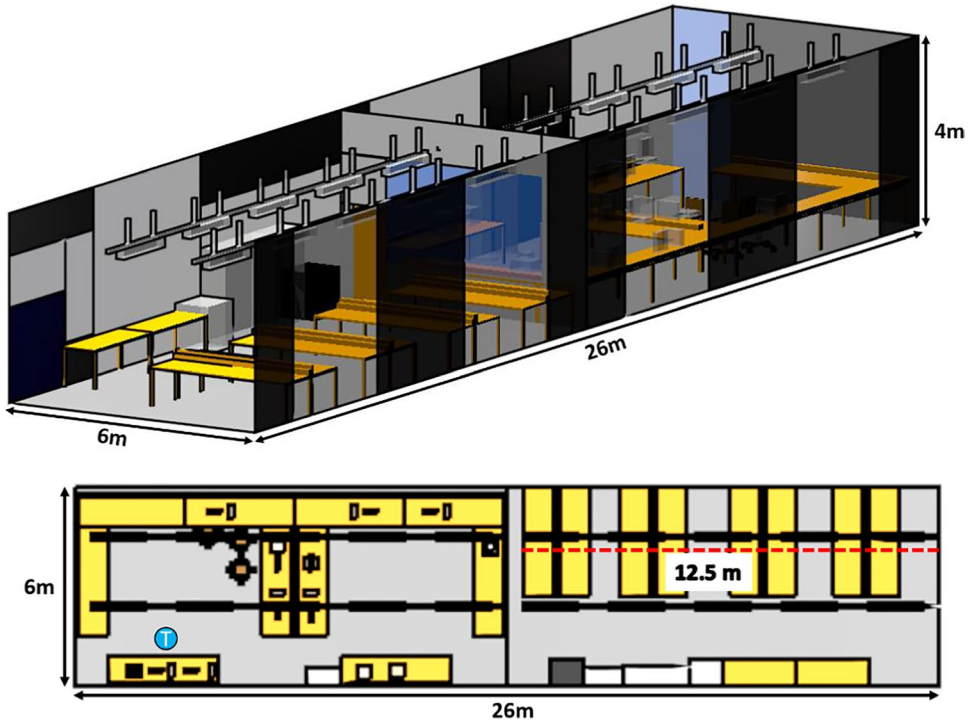

Fig. 1 Schematic representation of the scenario under test, corresponding to the Luis Mercader laboratory, Universidad Pública de Navarra. The figure depicts the simulation scenario implemented in the 3D RL simulation code, in which all furnishings and building structure elements have been considered

as follows: Section 2 describes the simulation methodology and the indoor scenario employed. Section 3 presents the wireless channel characterization results within the complete scenario volume, for received power level distributions, coverage/capacity estimations, signal to noise ratio maps and time domain characteristics considering systems operating

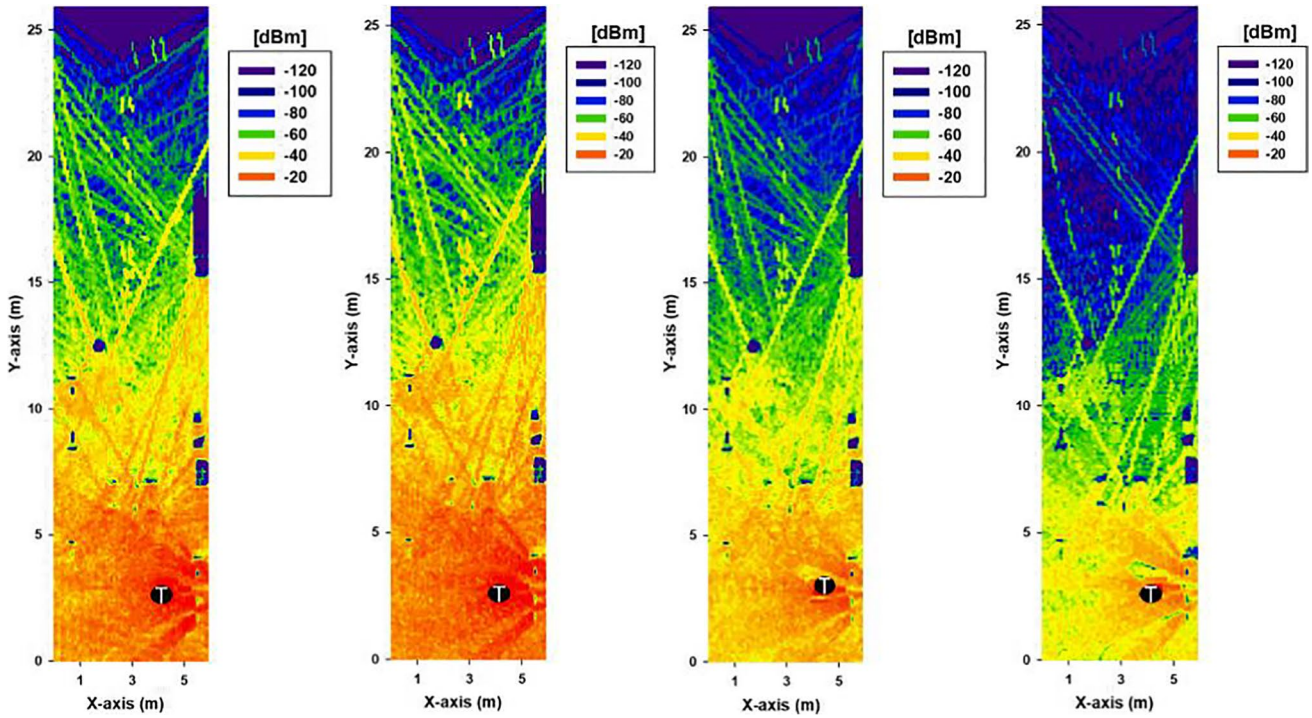

Fig. 2 Distribution of received power levels for bi-dimensional cut planes at height h = 1.2 m for 433 MHz, 868 MHz, 2.4 GHz and 3.5 GHz, respectively, for the transmitter test transmitter location indicated

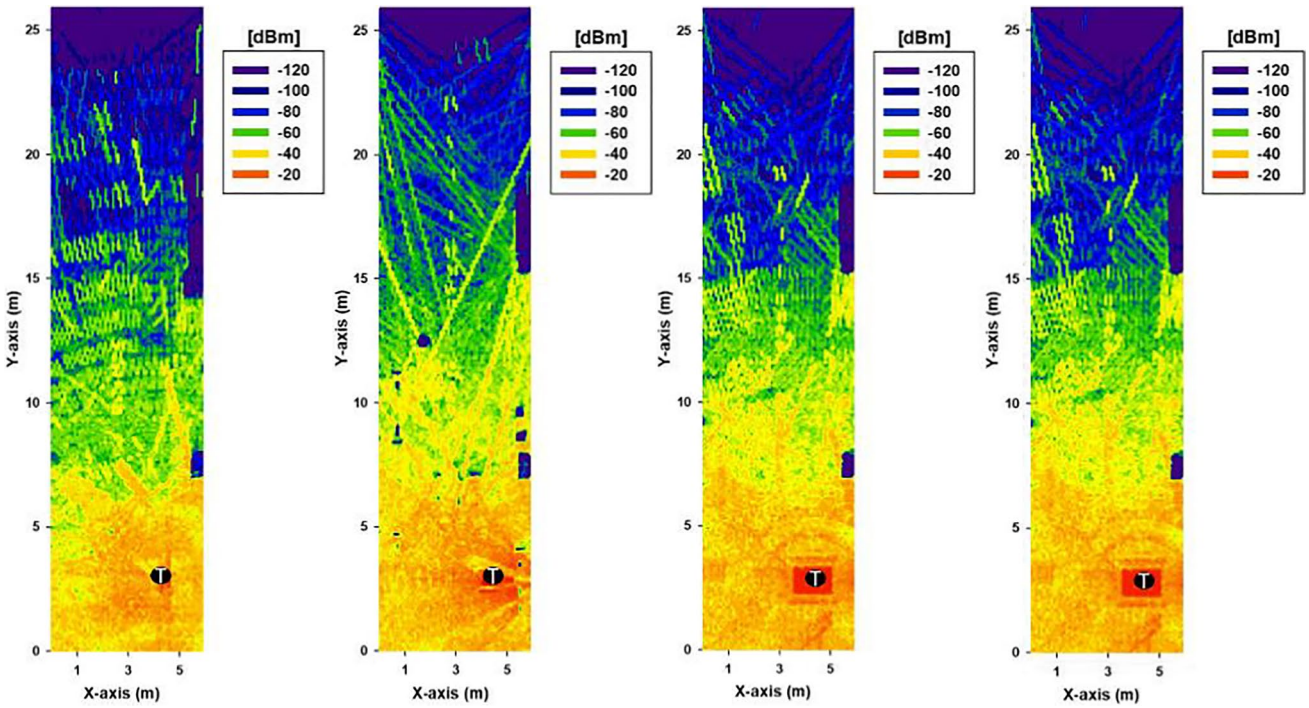

Fig. 3 Distribution of received power levels for bi-dimensional cut planes for an operation frequency of 2.4 GHz, for cut plane heights of 0.6 m, 1.2 m, 1.8 m and 2.4 m from the floor reference, respectively

within frequencies of 433 MHz, 868 MHz, 2.4 GHz and 3.5 GHz. Conclusions are presented in Section 4.

2 Simulation methodology and scenario description

Industrial scenarios in which wireless communication systems operate are generally characterized by exhibiting high density of multiple scatterers, high node density and arbitrary locations of interference sources. In order to provide accurate wireless channel characterization considering the impact of the aforementioned conditions, a deterministic approach based on geometric optics and uniform theory of diffraction (GO-UTD) is adopted in this work. An in-house simulation code has been implemented in Matlab, based in 3D Ray Launching (3D RL) approximation, in which transmitter sources are described by equivalent rays which depart from them in solid angular distribution. A comprehensive description of the code operation and mathematical

Fig. 4 Measurement scenario and setup within the Scenario under Test, located at the Luis Mercader laboratory, at the Public University of Navarra

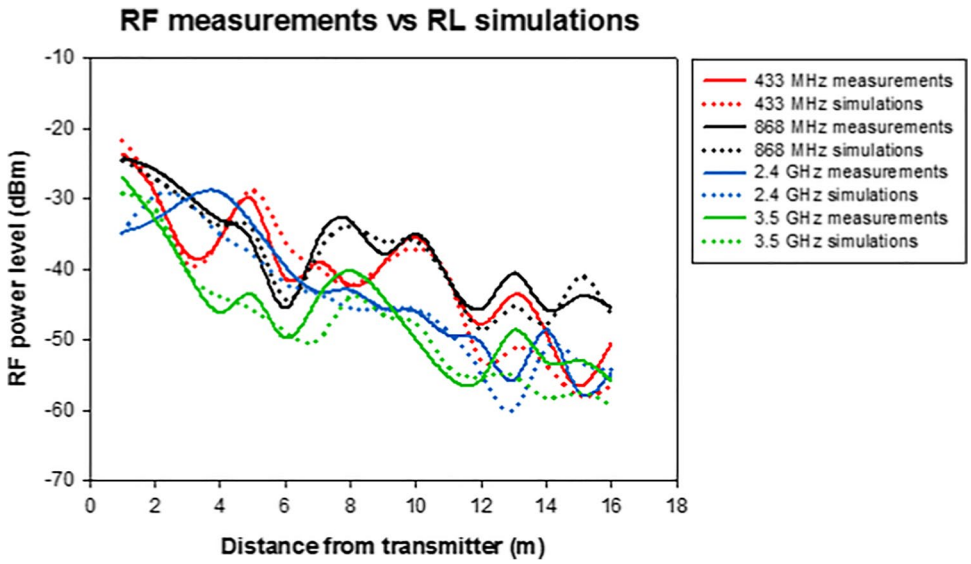

Fig. 5 Comparison between simulation and measurement results for linear TX-RX radials within the indoor scenario under analysis for CW frequencies of 433 MHz, 868 MHz, 2.4 GHz and 3.5 GHz

formulation is given in several references: a description of the 3D-RL computational technique and acceleration based in the use of feed-forward neural network interpolators is presented in [61]; in [62] and [63] the computational cost derived from the consideration of diffraction is reduced by applying electromagnetic diffusion principles; collaborative

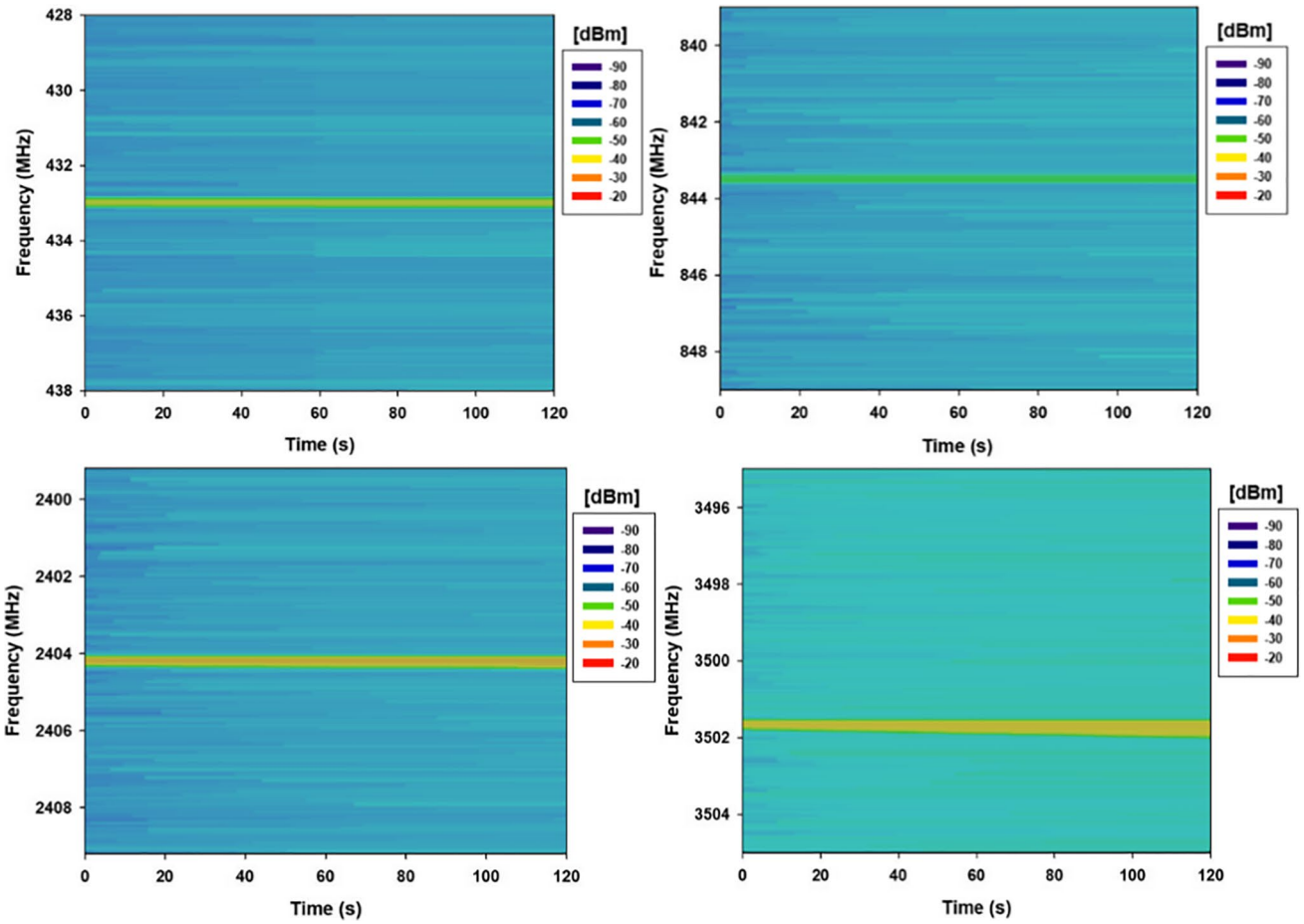

Fig. 6 Spectrogram measurements performed within the indoor scenario under analysis. A CW carrier has been activated at the center frequency of each frequency band as reference, for the frequency bands of 433 MHz, 868 MHz, 2.4 GHz and 3.5 GHz, respectively

filtering techniques in combination with the 3D RL code are considered in [64], to increase simulation resolution parameters in terms on number of launched rays and considered reflections; finally [65] provides a comprehensive description of convergence analysis criteria in terms of angular resolution, launched rays and maximum number of reflections considered. The simulation scenario is implemented in a 3D matrix, which is divided in cuboids. The elements within the scenario are described by their shape and size, as well as by the dispersive electromagnetic parameters of the constitutive materials, given by the dielectric constants and the electric conductivities. The material parameters employed are shown in Table 1.

Accuracy (related with average errors between estimation of simulated/measured received power levels as well as with time domain characterization) is mainly determined by the relation between cuboid size, subtended arc between transmitter and receiver points, angular resolution and the maximum amount of reflections allowed until ray extinction [65]. Additionally, edge diffraction as well as diffuse scattering can also be considered in the calculation. In this sense, extensive convergence analysis has been performed in relation with the 3D RL simulation code to obtain optimal values in terms of accuracy vs computational cost for simulation parameters such as angular resolution, cuboid size and maximum number of reflections until ray extinction [65]. The different parameters employed for the 3D RL simulations are given in Table 2. Computational complexity increases with scenario size as well as with the consideration of effects such as diffraction. To reduce computational cost for any given general scenario, the 3D RL code has been coupled to perform hybrid simulation, based on neural network ray interpolators [61], simplification aided by the consideration of electromagnetic diffusion [62, 63] or the use database enhanced estimations based on collaborative filtering techniques [64]. Parameters are dynamically adapted as a function of the scenario under analysis, which for the specific case of this work have made use of edge diffraction detection, owing to the type of clutter within the scenario.

In order to perform the analysis of wireless channel performance, the Luis Mercader laboratory, at the Universidad Pública de Navarra has been considered as the scenario under test. The schematic representation of this scenario is given in Fig. 1

The laboratory has a surface of 156 m^2 and a volume of 624 m^3, in which multiple work benches are present. The scenario has a large density of scatters, owing to constructive elements such as lighting and ducts, as well as obstruction owing to furniture and walls, qualitatively providing a scenario that resembles industrial operating conditions in

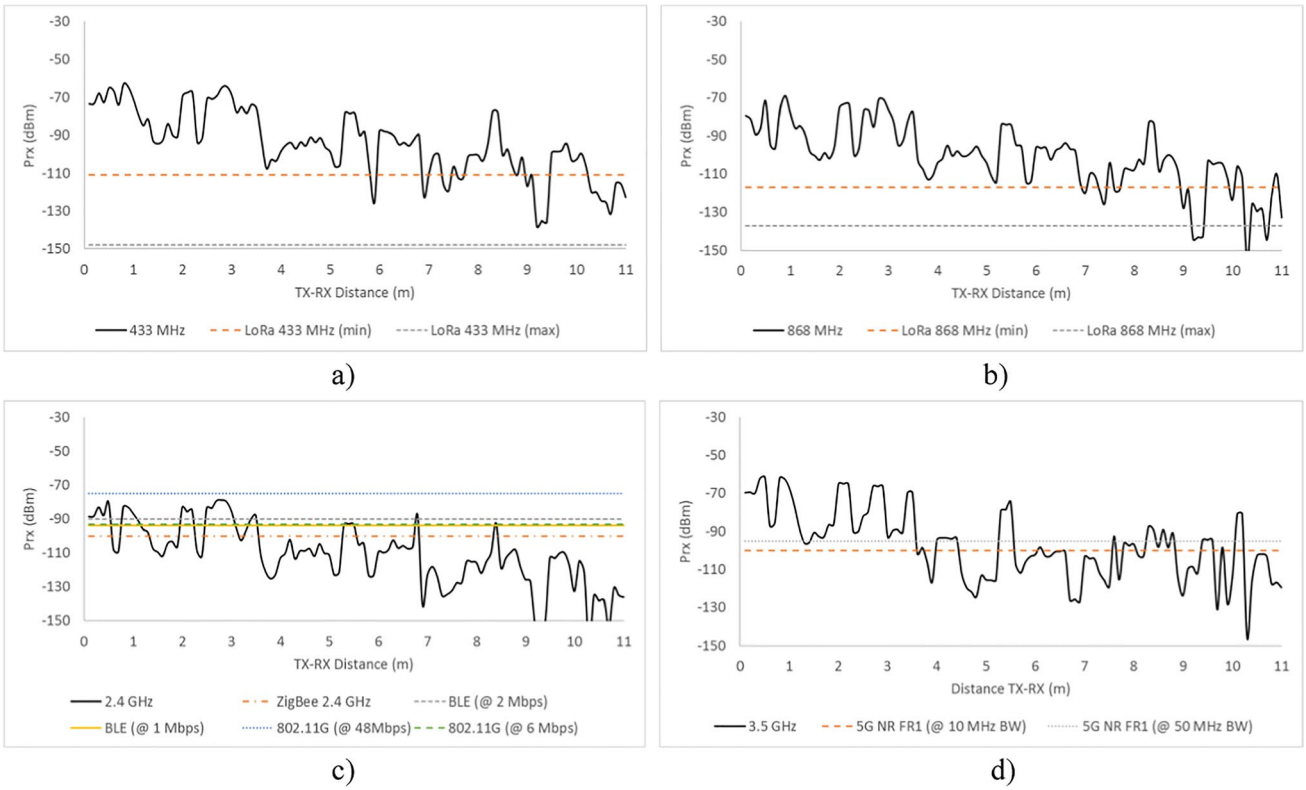

Fig. 7 Coverage/capacity estimations for linear TX-RX radials within the indoor scenario under analysis: **a** LoRa 433 MHz, **b** LoRa 868 MHz, **c** BLE, ZigBEE, 802.11G, **d** 5G FR1 NR

terms of the number of metallic scatterers, overall number of elements within the scenario and the proportions of line of sight, partial line of sight and non-line of sight channel condition. The lab is divided in two different sections by plaster/cement walls with large window openings. The schematic representation corresponds to the detailed simulation implemented within the 3D RL simulation code, in which the shapes, dimensions and material properties of all the constitutive elements have been mapped, following the information shown in Table 1. Different potential wireless transceiver locations and frequencies of operation will be considered within the volume of the scenario under test, as described in the following section.

3 Wireless channel characterization in complex indoor scenarios

Once the scenario under test has been defined, estimations of frequency/power distributions, coverage/capacity estimations, interference analysis and time domain parameters have been obtained. Different frequency bands have been analyzed, with the aim of considering LPWAN, WLAN and 5G NR FR1 system deployments. Simulation results for the complete volume of the scenario under analysis are obtained with the aid of 3D RL simulation code. It is worth noting that the complete topo-morphological details have been included in the recreated scenario, in order consider precisely the impact of all the elements within the scenario.

3.1 Coverage/capacity estimations within the indoor scenario

Initially, distributions of received power levels have been obtained for the aforementioned laboratory scenario. An equivalent transmitter source has been introduced within the scenario, operating in different frequency bands as a function of the systems under consideration (i.e., 433 MHz, 868 MHz, 2.4 GHz and 3.5 GHz. Results have been obtained for the complete volume of the indoor scenario under analysis, although in this work bi-dimensional distributions of

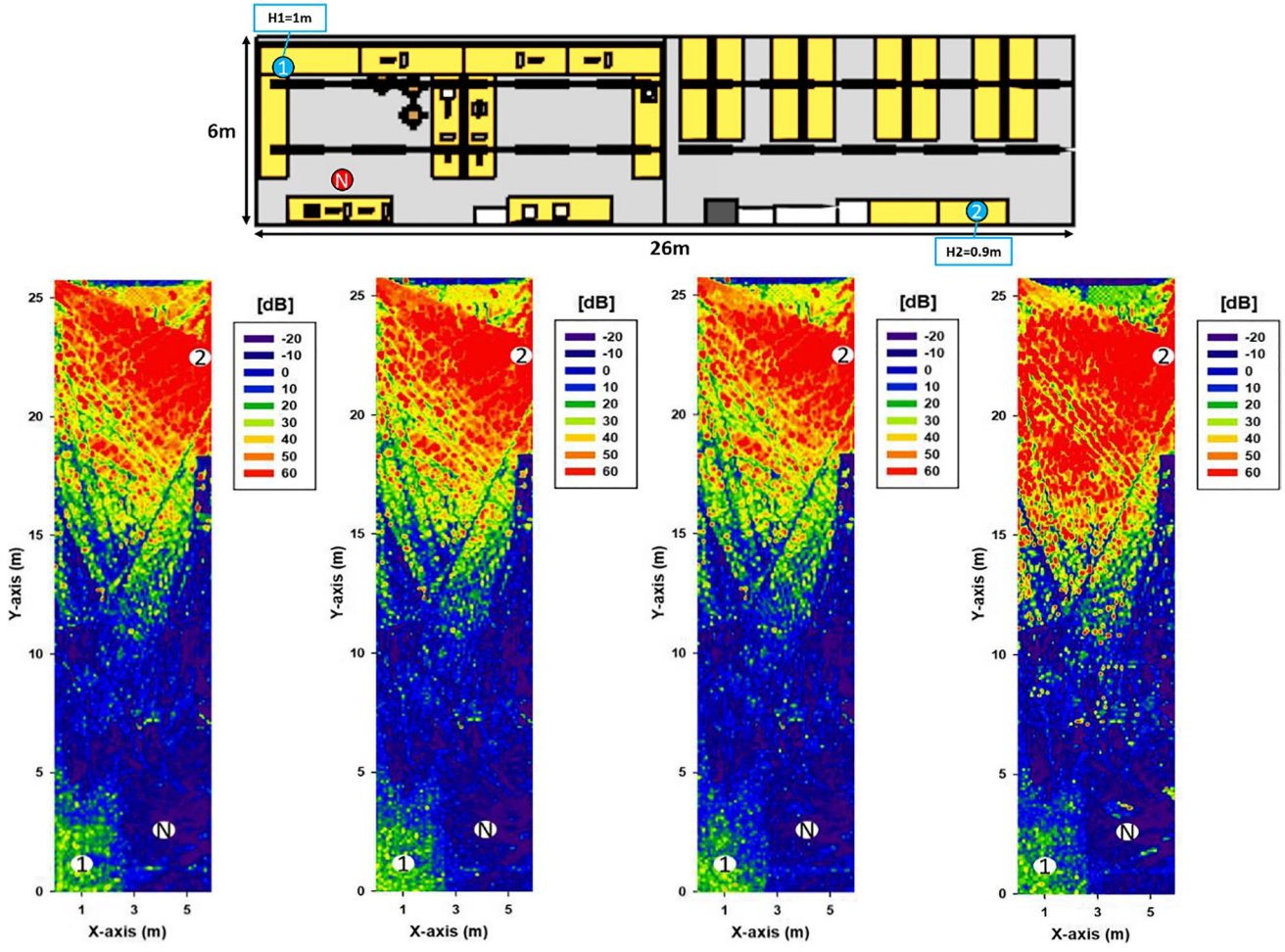

Fig. 8 Bi-dimensional distribution of SNR for cut-plane height of 1.2 m, for the case of two interference sources (with locations schematically depicted in the top image) for the case of 433 MHz, 868 MHz, 2.4 GHz and 3.5 GHz

received power levels are presented for different cut-plane heights for the sake of clarity. Figure 2 represents the results obtained for all the frequency bands under consideration for a height of h = 1.2 m from the floor reference. As it can be seen, as frequency increases, received power levels decrease owing to inherently higher path loss. Variations within the received power distribution are given by shadowing conditions in the case of NLOS paths, as well as by strong multipath components, which will be described in terms of time domain results later on. These effects can be seen by varying the observation cut-plane height, as depicted in Fig. 3, from 0.6 m to 2.4 m in regular 0.6 m intervals.

Validation of the estimations provided by the 3D RL simulation code have been obtained by performing continuous wave radio channel measurements within the scenario. To this extent, a wide band voltage-controlled oscillator (Mini-Circuits ZX95 VCO) has been connected to a wide band transmitter antenna (Antenova Omni LOG up to 8 GHz, depicted in Fig. 4), as transmit source.

Received power level measurement have been obtained with the aid of a portable spectrum analyzer (Rohde Schwarz FSH20, up to 20 GHz) directly connected to the same antenna model at the equivalent receiver end, which are depicted in Fig. 5. In all cases, simulation and measurement results are in good agreement, with average errors in the order of 3-5 dB for all cases, showing that the simulation approach provided accurate results for wireless channel estimation tasks.

The scenario has also been characterized in terms of pre-existent interference conditions. For this purpose, measured spectrograms have been obtained for each one of the measurement frequencies, with the receiver configuration previously described. A CW carrier for each frequency band of interest was to provide a reference value within the spectrograms, which can be clearly seen for the 4 frequency bands under consideration, depicted in Fig. 6. Average spectral power densities increase particularly in the case of

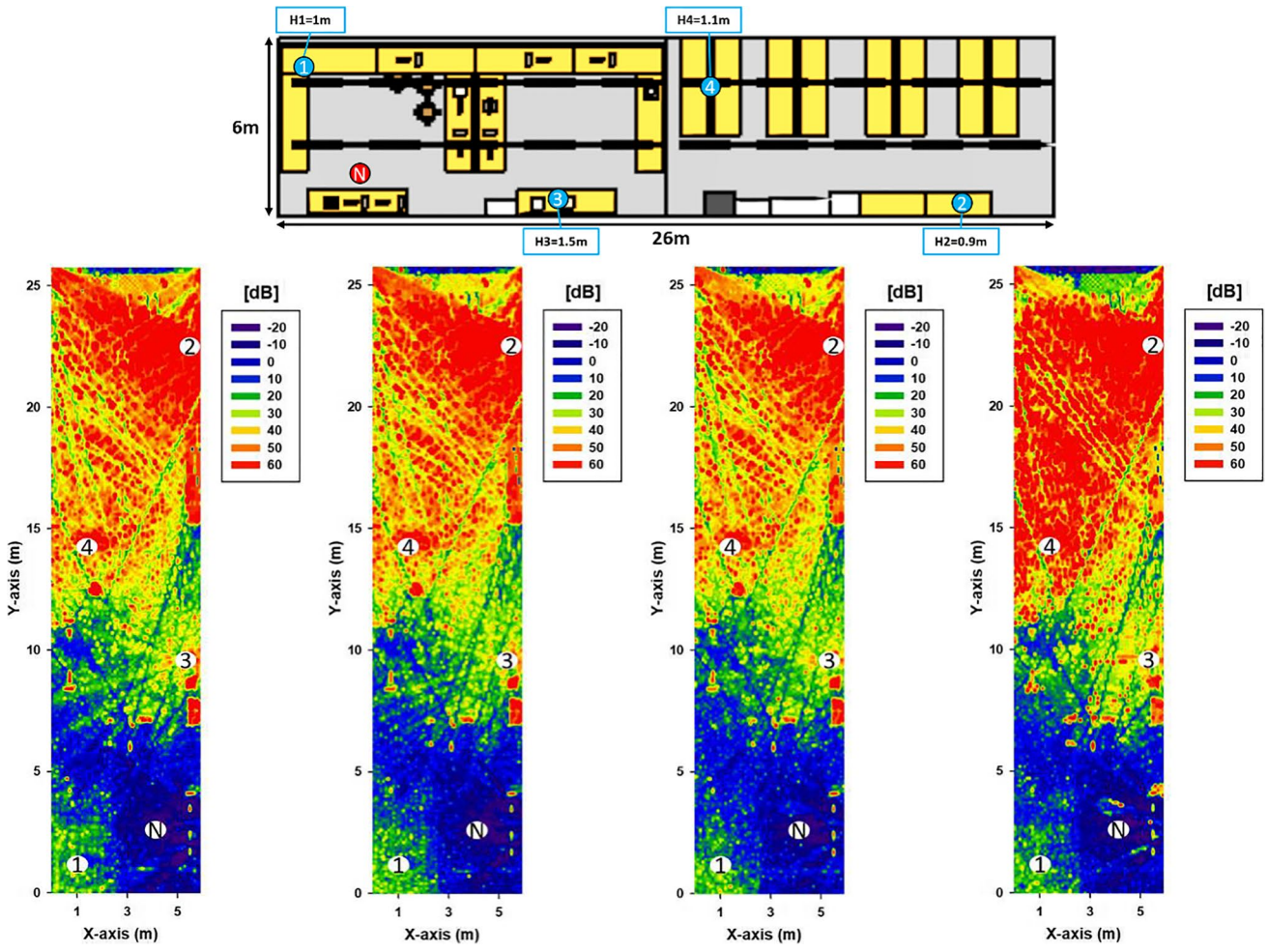

Fig. 9 Bi-dimensional distribution of SNR for cut-plane height of 1.2 m, for the case of four interference sources (with locations schematically depicted in the top image) for the case of 433 MHz, 868 MHz, 2.4 GHz and 3.5 GHz

2.4 GHz and 3.5 GHz, owing to pre-existent wireless systems (WLAN, WBAN and PLMN).

To gain insight in QoS and QoE performance, coverage/capacity estimations can be obtained, as a function of receiver sensitivity for adaptive modulation and coding schemes, thus providing variable sensitivity levels. The corresponding variations in coverage radius as a function of the system employed considering the effect of the surrounding indoor environment can be seen for different linear radial distributions, as shown in Fig. 7. Different systems have been considered: LoRa/LoRaWAN (@433 MHz, @868 MHz), BLE (@1 Mbps, @ 2 Mbps), WLAN (802.11 G @ 6 Mbps, @ 48 Mbps) and 5G NR FR1 3.5 GHz (@ BW 10 MHz, @ BW 50 MHz). Link balance results indicate that an increase in transmission rate, coverage radius decrease as a result in reduction in receiver sensitivity threshold. Moreover, significant variations, in excess of 20 dB for distance variations in the range of 10 cm owing to fast fading can be observed, with relevant link variations in the 1 m to 7 m range.

3.2 Interference analysis

Coverage/capacity relations are further constrained by variations in sensitivity owing to the pre-existent noise level within the scenario under analysis. Overall noise power spectral density is given by intra-system interference (i.e., additional transceiver operating within the host system), inter-system interference (operation and co-existence of external communication systems) and external interference sources (e.g., EMI related interference sources, such as motors or machines). The impact of interference has particular relevance in the case of context aware environments, owing to the need of increasing overall transceiver density, which is the case of IIoT applications.

To gain insight in relation with the joint impact of node density variation and the location of elements within the indoor scenario, distributions of SNR within the complete simulation volume have been obtained for the scenario under test. To this extent, different potential transceiver nodes have been located, varying their density from 2 to 8 nodes, for

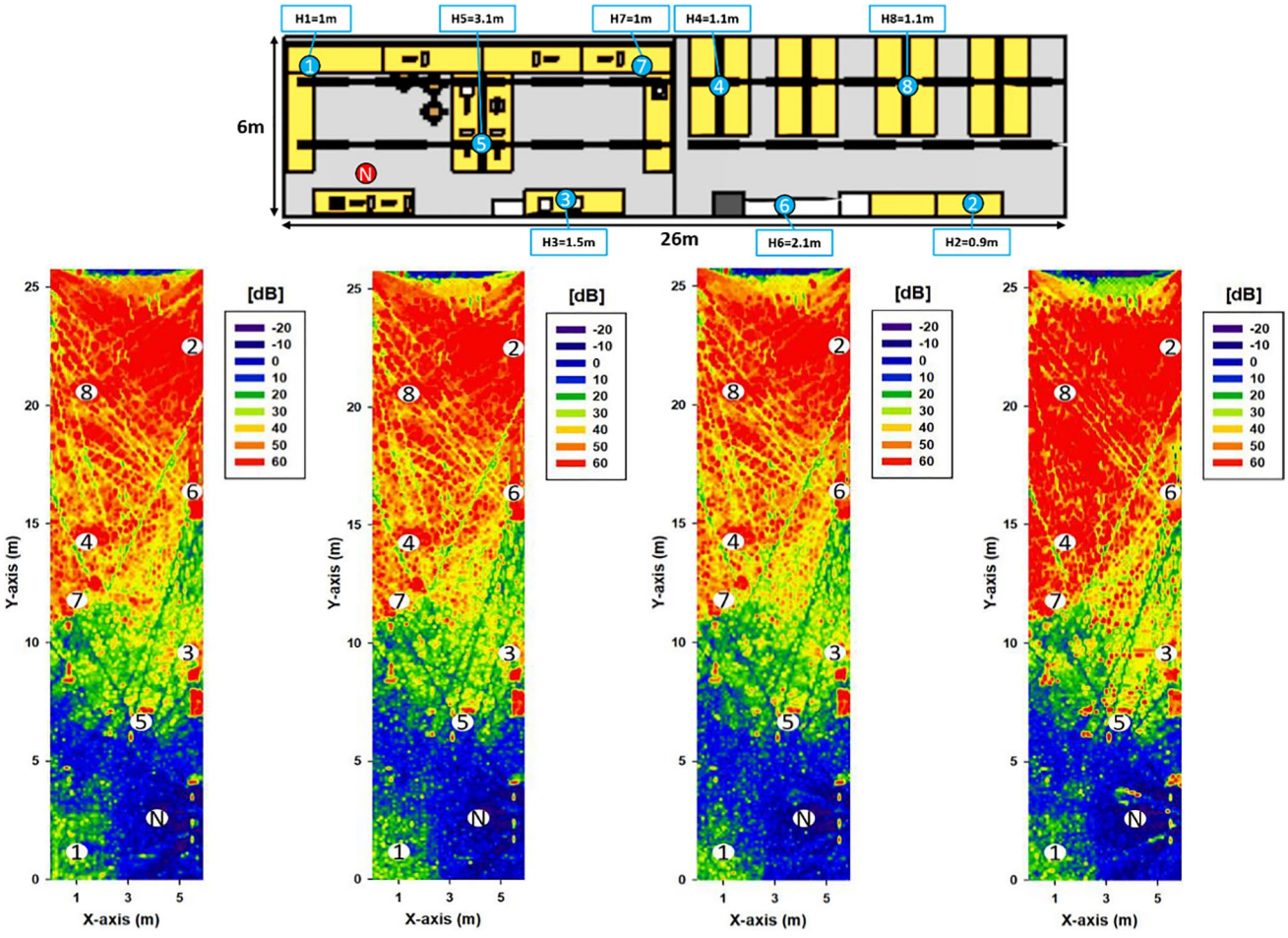

Fig. 10 Bi-dimensional distribution of SNR for cut-plane height of 1.2 m, for the case of eight interference sources (with locations schematically depicted in the top image) for the case of 433 MHz, 868 MHz, 2.4 GHz and 3.5 GHz

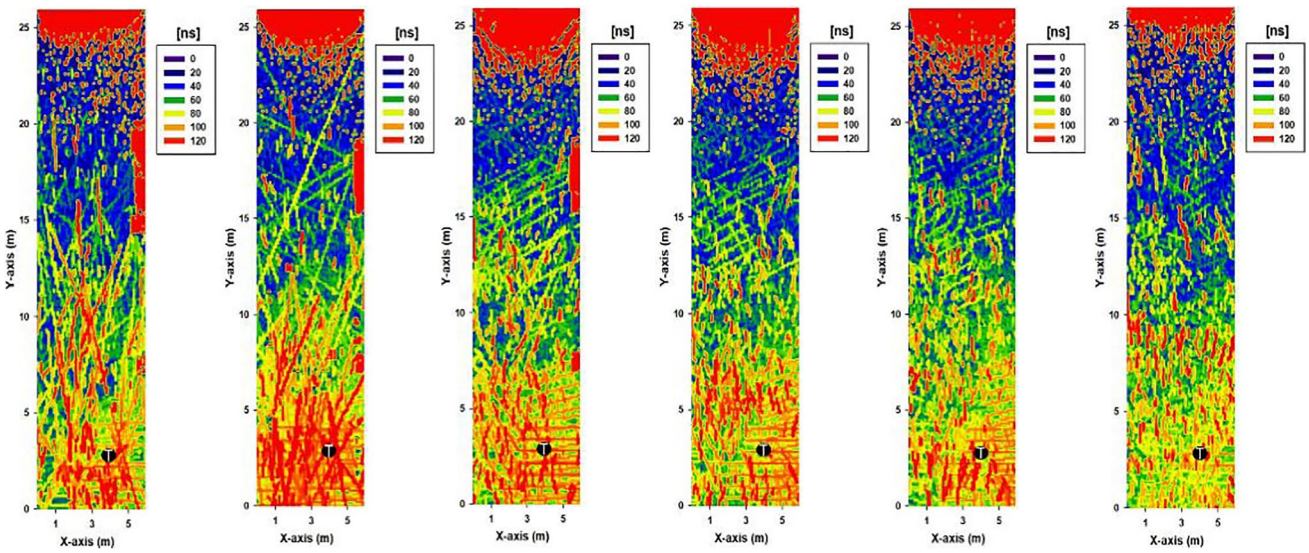

Fig. 11 Delay Spread Distributions for an operating frequency @433 MHz for cut-plane heights (left to right) of 0.6 m, 1.2 m, 1.8 m, 2.4 m, 3 m and 3.6 m, respectively

all the frequencies of operation, where node N is considered a potential interference source, with the aim of providing a generalizable channel characterization. Results for a given cut-plane height of h = 1.2 m are depicted in Fig. 8 (for the case of 2 transceiver nodes), Fig. 9 (for the case of 4 transceiver nodes) and Fig. 10 (for the case of 8 transceiver nodes). As a function of transceiver location, interference conditions change. In the case of the transceivers locates within the scenario, it is worth noting that their height in some cases vary as to consider potentially different locations as a function of node characteristics or application. Most of the nodes are within the 0.9 m-1.1 m range, coincident with the heights of the work benches. In the case of node #3, the height is 3.1 m and #6 the height is 2.1 m, corresponding to infrastructure nodes, exhibiting larger differences (especially in the case of node #3). An increase in the number of transceivers leads to smaller link distances, which can adapt to the existence of the interference node N owing to lower path losses. In any case, the presence of specific scatterers and large objects which lead to shadowing significantly modify SNR conditions (with average differences in excess of 5 dB for adjacent cuboids within the scenario), which can be observed with the aid of volumetric deterministic estimation.

3.3 Time domain characterization

In order to gain insight in relation with the influence of time domain characteristics in overall performance (e.g., delay metrics, coherence time or channel equalization features, among others), temporal parameters have also been estimated with the aid of 3D RL method. As an example, the estimation of delay spread, considering a fixed transmitter location (marked as T) has been obtained for the complete simulation volume. Figure 11 shows the results obtained, in the case of an operating frequency of 433 MHz for different cut-plane heights (of 0.6 m, 1.2 m, 1.8 m, 2.4 m, 3 m and 3.6 m, respectively). Variations in the specific cut plane heights lead to clearly visible variation in delay spread values, with variations in excess of 10 ns per cuboid in certain locations, owing to the contributions of the scatterer distribution to multipath propagation components.

The effect of multipath propagation can be observed in more detail by analyzing power delay profile (PDP) results obtained for locations within the indoor scenario. Several examples of PDPs have been obtained for the points indicated in Fig. 12. The case in which the frequency of operation of 433 MHz is employed is depicted in Fig. 13. All the

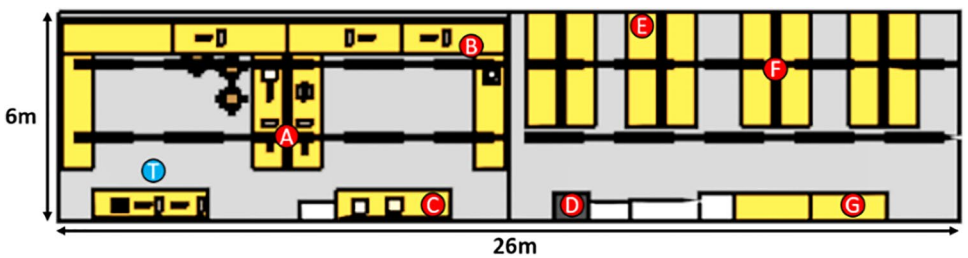

Fig. 12 Location of PDP estimation points within the indoor scenario under test

7 different observation points within the scenario have been considered. As it can be seen, there are relevant differences between the PDP estimations, with delay spreads varying from 35 ns to approximately 100 ns. There are also observable differences in the number of components detected, from 2 to over 30 components. This is directly related to the relative distance between the transmitter location T and the observation points. The further the observation point is (e.g., point #G), fewer components are detected, given by the maximum number of reflected rays (N = 6) allowed until ray extinction (fixed by 3D RL convergence analysis described in [65]).

Results have been obtained for all the operation frequencies and have been depicted (in this case only for points B and D) in Fig. 14. Differences can be observed mainly in detected power levels, which progressively decrease as frequency increases, as a consequence of increased path losses.

3.4 Discussion

Different received power level estimations have been obtained for the frequency bands spanning from 433 MHz to 3.5 GHz, obtaining 2D power level distributions as well as linear received power level radial. In this way, coverage/capacity results have been obtained considering different wireless communication systems operating within these bands as a function of receiver sensitivity values (LoRa/LoRaWAN, BLE, ZigBee, WLAN and 3G NR FR1), indicating relevant variations in achievable link distances, as a function of node location, node density and interference levels. Multipath propagation has also been characterized within the complete scenario volume, by means of delay dispersion as well as power delay profile estimation for different locations within the frequency bands under analysis. The results indicate strong variations in dispersion delay,

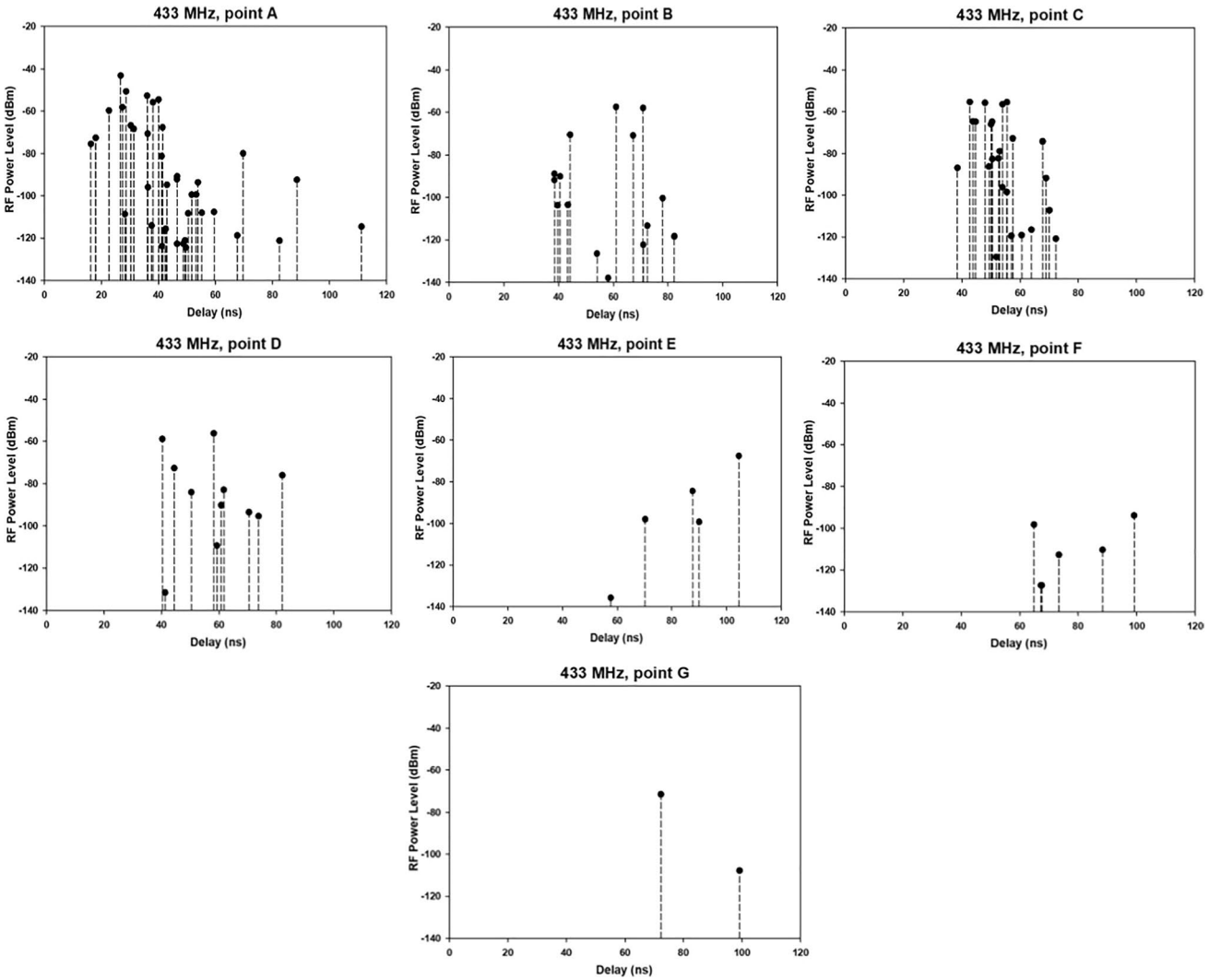

Fig. 13 Estimation of PDP, for the different points indicated in the scenario, at an operating frequency of 433 MHz

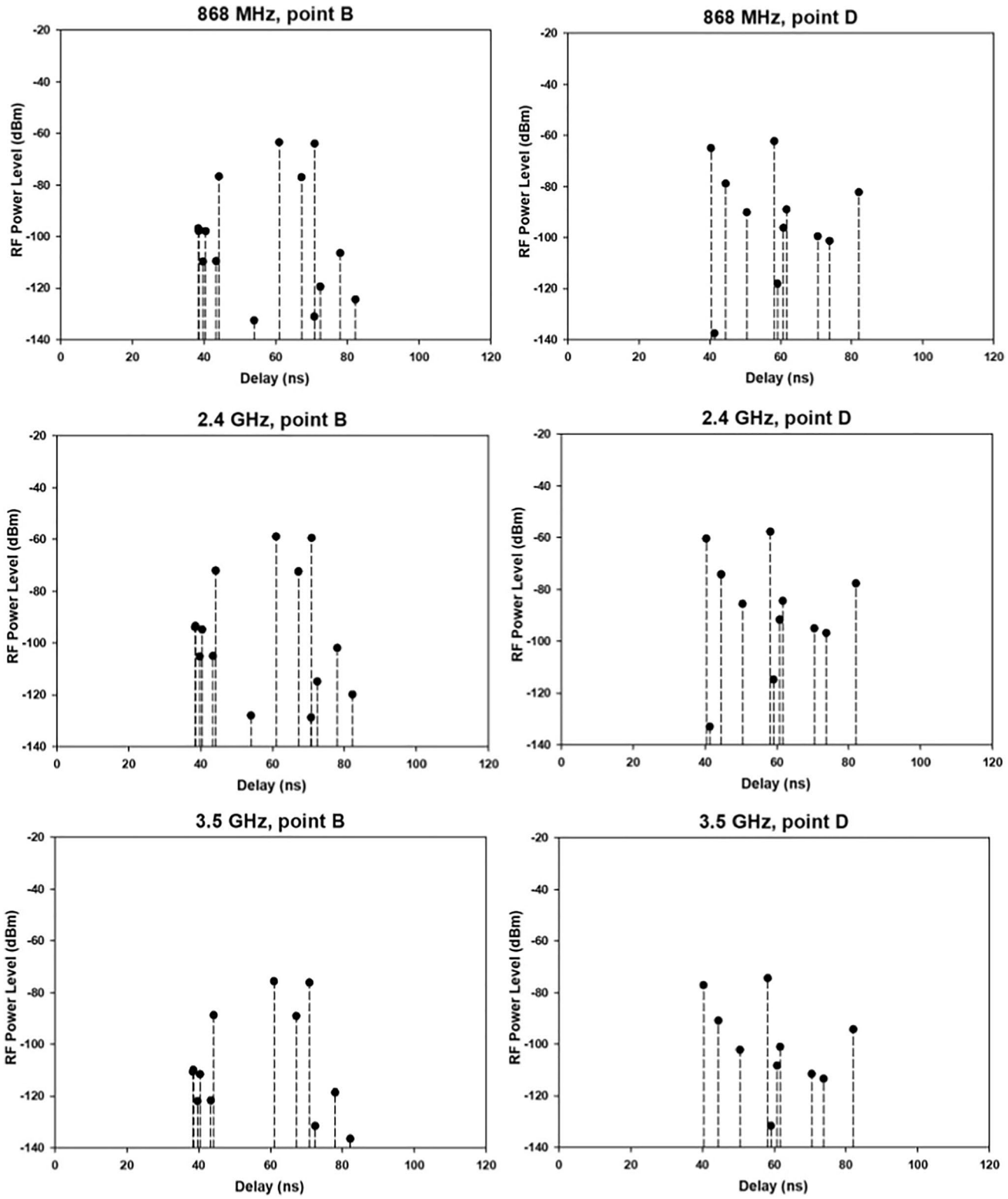

Fig. 14 Estimation of PDP, for the points B and D indicated in the scenario, at an operating frequency of 868 MHz (top), 2.4 GHz (middle) and 3.5 GHz (bottom)

with values ranging from 35 ns to over 100 ns within the scenario, which is directly linked with the presence of line of sight as well as partial line of sight and non-line of sight links within the scenario under test.

4 Conclusions

In this work, accurate wireless channel characterization within the complete volume of indoor scenarios, compatible with industrial environments, with high density of scatterers and objects has been presented. By means of an in-house implemented hybrid 3D Ray Launching simulation code, received power level distributions, coverage/capacity estimations, interference mapping and time domain characterization results have been obtained for 433 MHz, 868 MHz, 2.4 GHz and 3.5 GHz frequency bands within a complex indoor scenario, with high density of scatterers. Measurement results have been obtained for received power levels have been obtained, showing good agreement with simulation results for all frequency bands, with average errors below 3 dB.

The proposed deterministic 3D RL wireless channel approximation can aid in wireless device/system design and planning tasks, optimizing node location and configuration, in terms of QoS/QoE and energy consumption, considering the specific characteristics of indoor industrial environments. By applying the proposed deterministic channel modelling approach, the complete scenario volume is considered, enabling the location of transceivers at any given point of the scenario under test, as well as the consideration of arbitrary distributions of interference sources. In this way, flexible network topologies can be analyzed and envisaged enabling embedding wireless communication transceivers within the most optimal locations, as a function of the time/frequency coverage/capacity estimations. Future work considers dynamic channel characterization considering elements such as human body motion or the presence of unmanned industrial vehicles or complex interference distributions, among others.

Funding Open Access funding provided by Universidad Pública de Navarra. This work was supported by the European Union's Horizon 2020 research and Innovation programme under grant agreement N°774094 (Stardust-Holistic and Integrated Urban Model for Smart Cities) and by Ministerio de Ciencia, Innovación y Universidades, Gobierno de España (Agencia Estatal de Investigación, Fondo Europeo de Desarrollo Regional -FEDER-, European Union) under the research grant RTI2018-095499-B-C31 IoTrain.

Declarations

Conflicts of interest/Competing interests The authors declare no conflict of interest or competing interests.

References

1. Paniagua C, Delsing J (2021) Industrial Frameworks for Internet of Things: A Survey. IEEE Syst J 15(1):1149–1159. https://doi.org/10.1109/JSYST.2020.2993323
2. Vitturi S, Zunino C, Sauter T (2019) Industrial Communication Systems and Their Future Challenges: Next-Generation Ethernet, IIoT, and 5G. Proc IEEE 107(6):944–961. https://doi.org/10.1109/JPROC.2019.2913443
3. Dietrich S, May G, Hoyningen-Huene JV et al (2018) Frame Conversion Schemes for Cascaded Wired / Wireless Communication Networks of Factory Automation. Mobile Netw Appl 23:817–827. https://doi.org/10.1007/s11036-017-0881-2
4. MamadouMamadou A, Toussaint J, Chalhoub G (2020) Survey on Wireless Networks Coexistence: Resource Sharing in the 5G Era. Mobile Netw Appl 25:1749–1764. https://doi.org/10.1007/s11036-020-01564-w
5. Qiu T, Chi J, Zhou X, Ning Z, Atiquzzaman M and Wu DO (2020) Edge Computing in Industrial Internet of Things: Architecture, Advances and Challenges, in IEEE Communications Surveys & Tutorials. 22(4): 2462–2488, Fourthquarter. https://doi.org/10.1109/COMST.2020.3009103.
6. Aggarwal S, Kumar N (2019) Fog Computing for 5G-Enabled Tactile Internet: Research Issues, Challenges, and Future Research Directions. Mobile Netw Appl. https://doi.org/10.1007/s11036-019-01430-4
7. Hamidi-Sepehr F et al. 5G urLLC: Evolution of High-Performance Wireless Networking for Industrial Automation, in IEEE Communications Standards Magazine. https://doi.org/10.1109/MCOMSTD.001.2000035
8. Baumann D, Mager F, Wetzker U, Thiele L, Zimmerling M, Trimpe S (2021) Wireless Control for Smart Manufacturing: Recent Approaches and Open Challenges. Proc IEEE 109(4):441–467. https://doi.org/10.1109/JPROC.2020.3032633
9. Henningsen S, Dietzel S, Scheuermann B (2018) Misbehavior Detection in Industrial Wireless Networks: Challenges and Directions. Mobile Netw Appl 23:1330–1336. https://doi.org/10.1007/s11036-018-1040-
10. Zhu J, Zou Y, Zheng B (2017) Physical-Layer Security and Reliability Challenges for Industrial Wireless Sensor Networks. IEEE Access 5:5313–5320. https://doi.org/10.1109/ACCESS.2017.2691003
11. Tange K, De Donno M, Fafoutis X and Dragoni N (2020) A Systematic Survey of Industrial Internet of Things Security: Requirements and Fog Computing Opportunities, in IEEE Communications Surveys & Tutorials. 22(4):2489–2520, Fourthquarter. https://doi.org/10.1109/COMST.2020.3011208

12. Abdallah M, Dobre OA, Ho P-H, Jabbar S, Khabbaz MJ, Rodrigues JJPC (2020) Blockchain-Enabled Industrial Internet of Things: Advances, Applications, and Challenges. IEEE Internet of Things Magazine 3(2):16–18. https://doi.org/10.1109/MIOT.2020.9125425
13. Mao W, Zhao Z, Chang Z, Min G, Gao W. Energy Efficient Industrial Internet of Things: Overview and Open issues, in IEEE Transactions on Industrial Informatics. https://doi.org/10.1109/TII.2021.3067026.
14. Savazzi S, Nicoli M, Bennis M, Kianoush S, Barbieri L (2021) Opportunities of Federated Learning in Connected, Cooperative, and Automated Industrial Systems. IEEE Commun Mag 59(2):16–21. https://doi.org/10.1109/MCOM.001.2000200
15. Ahmad I et al (2021) The Challenges of Artificial Intelligence in Wireless Networks for the Internet of Things: Exploring Opportunities for Growth. IEEE Ind Electron Mag 15(1):16–29. https://doi.org/10.1109/MIE.2020.2979272
16. Chen K-C, Lin S-C, Hsiao J-H, Liu C-H, Molisch AF, Fettweis GP (2021) Wireless Networked Multirobot Systems in Smart Factories. Proc IEEE 109(4):468–494. https://doi.org/10.1109/JPROC.2020.3033753
17. Liu L, Han G, Shen J et al (2019) Diffusion Distance-Based Predictive Tracking for Continuous Objects in Industrial Wireless Sensor Networks. Mobile Netw Appl 24:971–982. https://doi.org/10.1007/s11036-018-1029-8
18. Wetzker U, Splitt I, Zimmerling M, Boano CA and Römer K (2016) Troubleshooting Wireless Coexistence Problems in the Industrial Internet of Things, 2016 IEEE Intl Conference on Computational Science and Engineering (CSE) and IEEE Intl Conference on Embedded and Ubiquitous Computing (EUC) and 15th Intl Symposium on Distributed Computing and Applications for Business Engineering (DCABES) pp. 98–98. https://doi.org/10.1109/CSE-EUC-DCABES.2016.167.
19. Ding Y et al. (2015) Experimental investigation of the packet loss rate of wireless industrial networks in real industrial environments," 2015 IEEE International Conference on Information and Automation, pp. 1048-1053. https://doi.org/10.1109/ICInfA.2015.7279441.
20. Li F, Lam KY, Sheng Z et al (2018) Q-Learning-Based Dynamic Spectrum Access in Cognitive Industrial Internet of Things. Mobile Netw Appl 23:1636–1644. https://doi.org/10.1007/s11036-018-1109-9
21. Cai H, Zhang Y, Yan H et al (2016) A Delay-Aware Wireless Sensor Network Routing Protocol for Industrial Applications. Mobile Netw Appl 21:879–889. https://doi.org/10.1007/s11036-016-0707-7
22. Montero S, Gozalvez J, Sepulcre M (2017) Link Scheduling Scheme with Shared Links and Virtual Tokens for Industrial Wireless Sensor Networks. Mobile Netw Appl 22:1083–1099. https://doi.org/10.1007/s11036-016-0727-3
23. Tuan NT, Kim D, Lee J (2018) On the Performance of Cooperative Transmission Schemes in Industrial Wireless Sensor Networks. IEEE Trans Industr Inf 14(9):4007–4018. https://doi.org/10.1109/TII.2018.2846671
24. Atat R, Liu L, Wu J et al (2019) Green Massive Traffic Offloading for Cyber-Physical Systems over Heterogeneous Cellular Networks. Mobile Netw Appl 24:1364–1372. https://doi.org/10.1007/s11036-018-0995-1
25. Dionísio R, Lolić T and Torres P (2020) Electromagnetic Interference Analysis of Industrial IoT Networks: From Legacy Systems to 5G, 2020 IEEE Microwave Theory and Techniques in Wireless Communications (MTTW). pp. 41-46. https://doi.org/10.1109/MTTW51045.2020.9245057
26. Landa I, Blázquez A, Vélez M, Arrinda A (2017) Impulsive radio noise levels interfering wireless systems up to 1 Ghz. Antennas Propag RF Technol Transp Auton Platforms 2017:1–5. https://doi.org/10.1049/ic.2017.0018
27. Jiang X, Shokri-Ghadikolaei H, Fischione C et al (2019) A Simplified Interference Model for Outdoor Millimeter-wave Networks. Mobile Netw Appl 24:983–990. https://doi.org/10.1007/s11036-018-1030-2
28. Grimaldi S, Mahmood A, Hassan SA, Gidlund M, Hancke GP (2021) Autonomous Interference Mapping for Industrial Internet of Things Networks Over Unlicensed Bands: Identifying Cross-Technology Interference. IEEE Ind Electron Mag 15(1):67–78. https://doi.org/10.1109/MIE.2020.3007568
29. Chiwewe TM, Mbuya CF, Hancke GP (2015) Using Cognitive Radio for Interference-Resistant Industrial Wireless Sensor Networks: An Overview. IEEE Trans Industr Inf 11(6):1466–1481. https://doi.org/10.1109/TII.2015.2491267
30. Block D, Töws D and Meier U (2016) Implementation of efficient real-time industrial wireless interference identification algorithms with fuzzified neural networks, 2016 24th European Signal Processing Conference (EUSIPCO) pp. 1738–1742. https://doi.org/10.1109/EUSIPCO.2016.7760546
31. Sheikh MU, Ruttik K, Jäntti R, Hämäläinen J (2021) Blockage and Ray Tracing Propagation Model in 3GPP Specified Industrial Environment. Int Conf Inf Netw (ICOIN) 2021:397–402. https://doi.org/10.1109/ICOIN50884.2021.9333909
32. Jiang T et al. 3GPP Standardized 5G Channel Model for IIoT Scenarios: A Survey, in IEEE Internet of Things Journal. https://doi.org/10.1109/JIOT.2020.3048992
33. Jaeckel S et al (2019) Industrial Indoor Measurements from 2–6 GHz for the 3GPP-NR and QuaDRiGa Channel Model, 2019 IEEE 90th Vehicular Technology Conference (VTC2019-Fall) pp. 1–7. https://doi.org/10.1109/VTCFall.2019.8891356
34. Liu Y, Wang Cx, Dai R, Guo X, Yu Y (2020) A General 3D Geometry-Based Stochastic Model for Industrial IoT Environments," 2020 IEEE Globecom Workshops (GC Wkshps, pp. 1–6. https://doi.org/10.1109/GCWkshps50303.2020.9367417
35. Chizhik D et al. (2020) Diffusion model for cluttered industrial environments at 28 GHz, 2020 IEEE International Symposium on Antennas and Propagation and North American Radio Science Meeting. pp. 1173-1174. https://doi.org/10.1109/IEEECONF35879.2020.9329874
36 Mohamed M, Cheffena M, Perez Fontan F, Moldsvor A (2018) A Dynamic Channel Model for Indoor Wireless Signals: Working Around Interference Caused by Moving Human Bodies. IEEE Antennas Propag Mag 60(2):82–91. https://doi.org/10.1109/MAP.2018.2796022
37. Challita F et al (2020) Massive MIMO Communication Strategy Using Polarization Diversity for Industrial Scenarios. IEEE Antennas Wirel Propag Lett 19(2):297–301. https://doi.org/10.1109/LAWP.2019.2960311
38. Xu H, Zhang R, Jiang Y and Zhai D (2019) Cross-Polarized Radio Propagation Measurement and Modelling in Temporal Domain for Factory Workshop Scenario, 2019 IEEE 20th International Conference on High Performance Switching and Routing (HPSR), pp. 1–6. https://doi.org/10.1109/HPSR.2019.8808100
39. Dupleich D, Müller R, Landmann M, Luo J, Galdo GD and Thomä RS (2020) Multi-band Characterization of Propagation in Industry Scenarios, 2020 14th European Conference on Antennas and Propagation (EuCAP), pp. 1–5. https://doi.org/10.23919/EuCAP48036.2020.9135630
40. Kun Z, Liu L, Cheng T, Ze Y and Jianhua Z (2019) Channel Measurement and Characterization for Industrial Internet of Things, 2019 IEEE Wireless Communications and Networking Conference (WCNC) pp. 1-5. https://doi.org/10.1109/WCNC.2019.8885930
41. Ozawa H, Fujimoto T, Katayama M (2018) Modeling of sub-GHz wave propagation in factories for reliable wireless communication,

2018 IEEE International Conference on Industrial Technology (ICIT). pp. 1598-1603. https://doi.org/10.1109/ICIT.2018.8352420
42. Syed NAA and Green PJ (2019) Wideband Communication Channel Sounding for Wireless Industrial Internet-of-Things Applications, 2019 IEEE VTS Asia Pacific Wireless Communications Symposium (APWCS), pp. 1-5. https://doi.org/10.1109/VTS-APWCS.2019.8851662
43. Narrainen J, D'Errico R (2019) Large Scale Channel Parameters in Industrial Environment, 2019 13th European Conference on Antennas and Propagation (EuCAP), pp. 1–5
44. Pereira MD, Romero RA, Fernandes N, de Sousa FR (2018) Pathloss and shadowing measurements at 2.4 GHz in a power plant using a mesh network, 2018 IEEE International Instrumentation and Measurement Technology Conference (I2MTC), pp. 1–6. https://doi.org/10.1109/I2MTC.2018.8409563
45. Kashef M, Candell R, Liu Y (2019) Clustering and Representation of Time-Varying Industrial Wireless Channel Measurements, IECON 2019 - 45th Annual Conference of the IEEE Industrial Electronics Society. pp. 2823–2829. https://doi.org/10.1109/IECON.2019.8926681
46. Katagiri K, Sato K, Inage K, Fujii T. Dynamic Radio Map Using Statistical Hypothesis Testing, in IEEE Transactions on Cognitive Communications and Networking. https://doi.org/10.1109/TCCN.2020.3047867
47. Li S, Zhao X, Gan J, Tang X, Zhang Y (2021) Measurement and Modeling of Wireless Channel Based on Broadband Micro-power System, 2021 6th International Conference on Intelligent Computing and Signal Processing (ICSP). pp. 720–724. https://doi.org/10.1109/ICSP51882.2021.9408969
48. Hou W, Du B, Wang Q, Du J, Zhang X (2021) Simulations and Analysis for Radio Wave Propagation Properties on 5G frequency Band in a Industrial Environment, 2021 IEEE 5th Advanced Information Technology, Electronic and Automation Control Conference (IAEAC), pp. 1019-1023. https://doi.org/10.1109/IAEAC50856.2021.9390599
49. Narrainen J, Makhoul G, D'Errico R (2019) Inter- and Intra-Cluster Characteristics of MIMO Industrial Channels, 2019 IEEE International Symposium on Antennas and Propagation and USNC-URSI Radio Science Meeting, pp. 2113-2114. https://doi.org/10.1109/APUSNCURSINRSM.2019.8888701
50. Adegoke EI, Edwards RM, Whittow WG, Bindel A (2019) Characterizing the Indoor Industrial Channel at 3.5GHz for 5G, 2019 Wireless Days (WD), pp. 1–4. https://doi.org/10.1109/WD.2019.8734160
51. Wassie DA, Rodriguez I, Berardinelli G, Tavares FML, Sorensen TB, Mogensen P (2018) Radio Propagation Analysis of Industrial Scenarios within the Context of Ultra-Reliable Communication, 2018 IEEE 87th Vehicular Technology Conference (VTC Spring), pp. 1–6. https://doi.org/10.1109/VTCSpring.2018.8417469
52. Cano C, Sim GH, Asadi A, Vilajosana X (2021) A Channel Measurement Campaign for mmWave Communication in Industrial Settings. IEEE Trans Wireless Commun 20(1):299–315. https://doi.org/10.1109/TWC.2020.3024709
53. Solomitckii D, Orsino A, Andreev S, Koucheryavy Y, Valkama M (2018) Characterization of mmWave Channel Properties at 28 and 60 GHz in Factory Automation Deployments, 2018 IEEE Wireless Communications and Networking Conference (WCNC), pp. 1-6. https://doi.org/10.1109/WCNC.2018.8377337
54. Razzaghpour M et al (2019) Short-Range UWB Wireless Channel Measurement in Industrial Environments, 2019 International Conference on Wireless and Mobile Computing, Networking and Communications (WiMob), pp. 1–6. https://doi.org/10.1109/WiMOB.2019.8923145
55. Li Q, Zhang N, Cheffena M, Shen X (2020) Channel-Based Optimal Back-Off Delay Control in Delay-Constrained Industrial WSNs. IEEE Trans Wireless Commun 19(1):696–711. https://doi.org/10.1109/TWC.2019.2948156
56. Van Haute T, Verbeke B, De Poorter E, Moerman I (2017) Optimizing Time-of-Arrival Localization Solutions for Challenging Industrial Environments. IEEE Trans Industr Inf 13(3):1430–1439. https://doi.org/10.1109/TII.2016.2550531
57. Wang L et al (2017) Channel characteristics analysis in smart warehouse scenario, 2017 IEEE International Symposium on Antennas and Propagation & USNC/URSI National Radio Science Meeting, pp. 1417-1418. https://doi.org/10.1109/APUSNCURSINRSM.2017.8072751
58. Messier GG, Wasson MW, Herrmann MJ (2017) Petroleum Refinery Mesh Network Propagation Measurements. IEEE Trans Antennas Propag 65(10):5645–5648. https://doi.org/10.1109/TAP.2017.2734170
59. Liu L, Zhang K, Tao C, Zhang K, Yuan Z, Zhang J (2018) Channel measurements and characterizations for automobile factory environments, 2018 20th International Conference on Advanced Communication Technology (ICACT), pp. 234–238. https://doi.org/10.23919/ICACT.2018.8323708
60. Chrysikos T, Georgakopoulos P, Oikonomou I, Kotsopoulos S (2018) Measurement-based characterization of the 3.5 GHz channel for 5G-enabled IoT at complex industrial and office topologies, 2018 Wireless Telecommunications Symposium (WTS), pp. 1–9. https://doi.org/10.1109/WTS.2018.8363946
61. Azpilicueta L, Rawat M, Rawat K, Ghannouchi FM, Falcone F (2014) 'A ray launching-neural network approach for radio wave propagation analysis in complex indoor environments.' IEEE Trans Antennas Propag 62(5):2777–2786
62. Azpilicueta L, Falcone F, Janaswamy R (2017) 'A hybrid ray launching-diffusion equation approach for propagation prediction in complex indoor environments.' IEEE Antennas Wireless Propag Lett 16:214–217
63. Azpilicueta L, Falcone F, Janaswamy R (2019) Hybrid Computational Techniques: Electromagnetic Propagation Analysis in Complex Indoor Environments. IEEE Antennas Propag Mag 61(6):20–30. https://doi.org/10.1109/MAP.2019.2943297
64. Casino F, Azpilicueta L, Lopez-Iturri P, Aguirre E, Falcone F, Solanas A (2017) 'Optimized wireless channel characterization in large complex environments by hybrid ray launching collaborative filtering approach.' IEEE Antennas Wireless Propag Lett 16:780–783
65. Azpilicueta L, Rawat M, Rawat K, Ghannouchi F, Falcone F (2014) Convergence Analysis in Deterministic 3D Ray Launching Radio Channel Estimation in Complex Environments. ACES Journal 29(4):256–271